
http://www.diva-portal.org

Postprint

This is the accepted version of a paper presented at *IEEE International Conference on RFID (RFID)*.

Citation for the original published paper:

Padmal, M., Rohner, C., Augustine, R., Voigt, T. (2023)
RFID Tags as Passive Temperature Sensors
In: *17th annual international conference on RFID, Seattle, WA, USA, June 13-15, 2023*.
(pp. 48-53).
IEEE International Conference on RFID
https://doi.org/10.1109/RFID58307.2023.10178523

N.B. When citing this work, cite the original published paper.

Permanent link to this version:
http://urn.kb.se/resolve?urn=urn:nbn:se:uu:diva-508480

RFID Tags as Passive Temperature Sensors

Madhushanka Padmal*, Christian Rohner*, Robin Augustine*, Thiemo Voigt*†
*Uppsala University, Sweden. †RISE Computer Science, Sweden.
madhushanka.padmal@angstrom.uu.se, christian.rohner@it.uu.se, {robin.augustine, thiemo.voigt}@angstrom.uu.se

***Abstract*—Temperature sensing and monitoring play a vital role in various applications. Non-invasive, item-level temperature sensing methods that require no direct line of sight with the measuring object are attractive. This paper presents such a temperature sensing method using commodity RFID tags with no infrastructure changes. RFID tags are widely deployed for product identification purposes. We explore the possibility of leveraging the RSSI measurements from commodity RFID tags for temperature sensing. Essentially, we model a relationship between the temperature and the relative permittivity of a material in terms of RSSI. Our method can measure temperature in the range of 22°C to 60°C and achieves a measurement accuracy of 2°C with a mean error of 1.5°C.**

***Index Terms*—Passive RFID, Temperature Sensing, RSSI**

I. Introduction

Temperature is a measure of thermal energy. The measurement of temperature has been an essential part of human life, with various applications ranging from life-critical medical applications to day-to-day activities. Monitoring the skin temperature under a plaster cast is a method to detect possible skin irritations [1]. The increase in human body temperature by a few degrees calls for medical care [2]. Keeping a baby formula at the correct temperature preserves its nutrition [3].

The basic principles used to measure temperature are the expansion of liquids or solids, the changes in electrical properties, or infrared radiation. Thermometers measure and quantify the temperature using a standard temperature scale such as Celsius and Kelvin [4]. There are several types of thermometers in use, such as alcohol thermometers, digital thermometers, and IR thermometers. They base on the principle of thermal equilibrium that requires non-blocking direct line of sight or contact with the measuring object which causes thermal energy leakage changing the temperature undesirably [4]. For example, opening a sealed box to measure the temperature of an item inside would change its temperature. Opening a bandaged wound to check its temperature will bruise the wound again. Hence a non-invasive, item-level temperature sensing method that requires no direct line of sight with the measuring object will greatly benefit such applications.

A straightforward method is to use a battery-powered wireless temperature meter mounted inside the enclosed space. This will transmit temperature readings to an external receiver. However, this does not enable item-level temperature measurements. Such sensors also require configuration and maintenance with replenishing batteries adding more overhead [5].

Radio Frequency Identification (RFID) systems have been widespread with billions of low-cost tags that are small and battery-less with a communication range of up-to 12 m [6], [7]. RFID tags can be uniquely identified and queried using an RFID reader that may or may not be in direct line of sight [7]. RFID tags on products are still readable even after the purchase. These factors make these tags easy to deploy and maintain and a viable candidate to reuse as non-invasive item-level temperature sensors.

There are two approaches to use commodity RFID tags as temperature sensors. The first is to embed a miniaturized temperature sensor on the RFID tag. Redesign of tags, however, is expensive and does not consider tags in the stores. The second approach reuses deployed and commodity RFID tags. This approach measures a signal property or a value backscattered from an RFID tag to estimate temperature. The biggest challenge with this approach is that environmental conditions and the setup heavily influence radio signals [8].

In this paper, we propose a non-invasive, item-level temperature sensing method that requires no direct contact with the measuring object using commodity RFID tags. We leverage the Received Signal Strength Indicator (RSSI), readily available from RFID reader's query output and map it using the thermal cooling curve of an item. The mapping between RSSI and the cooling curve reads temperature as a measure of RSSI. Our method achieves a measurement accuracy of 2°C over a temperature range of 22°C to 60°C with 1.5°C mean error.

II. Related Work

Temperature sensing using RFID tags has been in research for many years resulting in both commercially available products as well as academic research [5], [9]–[16].

Some commercial RFID tags are exclusively used as temperature sensors [9], [10]. RFM3200 is a standard compatible RFID temperature sensing tag with ± 2°C accuracy that costs around $3.5 [10]. Avery Dennison also has a line of passive RAIN RFID temperature sensing tags that cost around $0.3 [9]. These tags require specialized infrastructure and readers to measure temperature, leaving out low-cost general purpose RFID tags or reusing commodity tags on products.

There are multiple attempts in the literature to design temperature sensors using commodity RFID tags. Wang et al. propose to modify a commodity Alien Squiggle general-purpose RFID tag to build a temperature sensor [12]. They achieve >10°C accuracy by measuring the relative power difference to activate a modified tag and an unmodified tag. RTSense by Swadhin et al. use two RFID tags with custom designed antennas to estimate temperature using phase changes [13]. They achieve 2.9°C mean error and a read range of 3.5 m independent of the environment. Capdevila

979-8-3503-3551-4/23/$31.00 ©2023 IEEE

et al. explore the possibility of using passive RFID tags for sensing purposes [11]. They measure the reflection coefficient of two antenna impedance states of a matched tag antenna. They observe a close-linear relationship of phase variation with temperature. These solutions require modifications to the antenna, making them incompatible with commodity tags.

Xingyu et al.'s Thermotag estimates temperature by measuring the discharging period of a capacitor connected with the tag's state storing volatile memory [5]. Using this method, they achieve temperature readings with a mean error of 2.7°C in a range from 0°C to 85°C. Xiangyu et al.'s RFThermometer is a tensor-based compensation mechanism that uses phase readings from RFID tags to estimate the tag temperature. They achieve a mean measurement error of 5°C in a static environment [15]. These solutions require complex processing steps and reader interfaces to extract information such as tag states and phase from the RFID reader. In contrast, our solution requires only the RSSI measurements from a tag response that is readily available from any RFID reader interface.

Apart from these advanced measuring techniques, RFID tags have been reused in many passive sensing applications. Bhattacharyya et al. use two RFID tags to monitor if a package is refrozen by comparing the signal strength between the tags [16]. Unsoo et al. investigate how food quality affects the resonance frequency of an RFID tag to detect food contamination [8]. This requires multiple wideband antennas and heavily depends on the container and the environment. Vaz et al. present a long range RFID temperature sensor designed using standard CMOS process [17]. It works in the range of 35°C to 45°C with a 0.035°C resolution and 0.1°C accuracy. Custom tags are, however, expensive and difficult to deploy compared to the commodity RFID tags we use in our work.

III. System Design

Most commodity RFID tags have patch antennas. Surface properties such as permittivity and material thickness change the antenna impedance by weak coupling and affect both the reflecting and absorbing signals [18]. The weak coupling phenomenon occurs with materials even when they are not in direct contact with the antenna [19]. As an example, a patch antenna on a water-filled glass container couples with the water medium, and the water permittivity affects the antenna impedance. The temperature of a material has a direct relationship to its relative permittivity. Catenaccio et al. relate temperature with relative permittivity $\varepsilon(T)$ of water at temperature T in Kelvin as follows [20]:

$$\varepsilon(T) = 5321 \times T^{-1} + 233.76 - 0.9297 \times T + 0.1417 \times 10^{-2} \times T^{2} - 0.8292 \times 10^{-6} \times T^{3}. \quad (1)$$

The relative permittivity of water changes from approximately 88 to 55 when the temperature changes from 0°C to 100°C. A linear relationship between permittivity and temperature in the above ranges would yield 0.33 units of permittivity change per 1°C. Therefore, we investigate the impact of permittivity on patch antennas and relate it to temperature sensing using the antenna of an RFID tag. While others have used phase angles measurements and RFID tag states [5], [11]–[13], we propose to measure the RSSI. This would allow a simple measurement system that all RFID reader interfaces support. In the following, we perform initial simulations to evaluate how well an RFID patch antenna transmits signals when the permittivity of the surface changes.

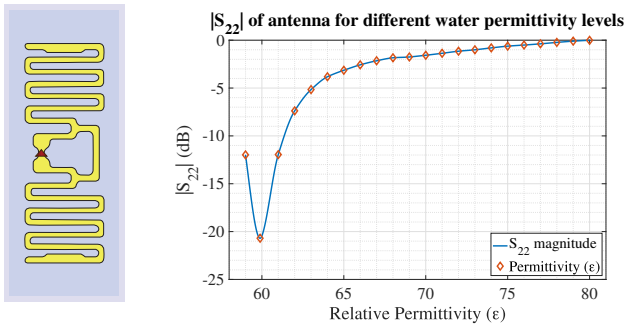

(a) Simulation model of RFID tag in CST.

(b) Output port reflection coefficient (S_{22}) of CST antenna simulation model for different water permittivity levels correspond to 22°C-85°C temperature range.

Fig. 1. Simulation results from CST Studio for RFID tag antenna performance under different water permittivity levels at 868 MHz. Higher temperatures decrease and lower temperatures increase the relative permittivity of water.

A. Simulation

We simulate an RFID patch antenna for a range of surface permittivity levels to investigate if there is a significant difference in performance. Fig. 1 (a) shows the tag antenna model in the CST Studio antenna simulation software [21]. We design the antenna model on a stack of glass and water layers resembling a glass container filled with water. Using (1), we calculate the relative permittivity for water in the temperature range from 22°C to 85°C, corresponding to room temperature and maximum operating temperature of an RFID tag [22], respectively. We use these calculated permittivity values as a parameter for the water layer in the simulation to simulate the changes in the output port reflection coefficient (S_{22}) of the antenna. The S_{22} parameter measures how much signal is reflected from the antenna output. Fig. 1 (b) shows the simulation results for the S_{22} of the antenna at 868 MHz operating frequency. Lower S_{22} corresponds to better antenna performance. Fig. 1 (b) shows the lowest reflection coefficient when ε is about 60, corresponding to ∼83°C. Interestingly, the exponential increase of the S_{22} curve for $\varepsilon > 60$ corresponding to temperatures lower than 83°C compensates each other with the temperature curve of a hot water bottle cooling down that we experimentally measure which follows Newton's law of cooling [23]. This is a beneficial property for our work.

Newton's law of cooling defines how fast a material cools down in the absence of an active heat source. The temperature $T(t)$ of a material at a given time t is

$$T(t) = T_a + (T_0 - T_a)e^{kt} \quad (2)$$

where T_a is the ambient temperature, T_0 is the initial temperature and k is the thermal conductivity [23]. Nagasaka et al. measure k experimentally for different liquids [24].

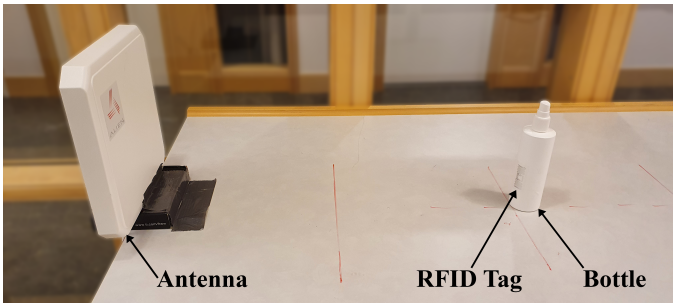

Fig. 2. Experiment setup with Impinj R420 RFID reader and Alien ALR-8611-AC antenna. The RFID tag is pasted on a bottle filled with hot water. The bottle is placed at a known distance from the antenna centerline.

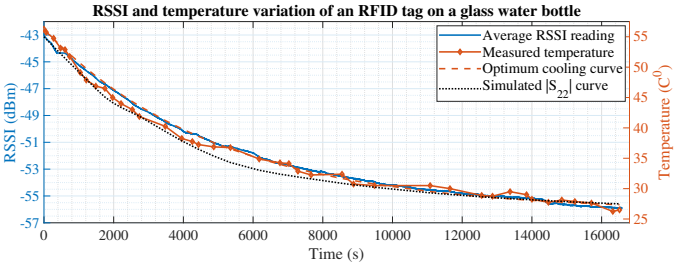

Fig. 3. RSSI variation of an RFID tag (model RF600600) with actual temperature readings. We plot a vertically scaled portion of the related S_{22} curve from CST simulation on the same figure with a dotted black line. This corresponds to $\varepsilon \in [77.4, 69.5]$ for temperature (°C) [27.9, 54.9] respectively.

The simulation results show a significant performance difference in the RFID patch antenna when the surface permittivity changes from 59 to 80. Our result shows that when the water temperature changes from 83°C to 20°C, the output signal strength from the antenna degrades exponentially.

B. Basic experiment

We conduct an experiment to verify the simulated antenna behavior from the previous experiment with a real experiment. We use an Impinj R420 RFID reader with Alien ALR-8611-AC antenna [25] to investigate the performance of an RFID tag antenna in terms of RSSI. The RFID tag is pasted on a bottle filled with hot water and placed in front of the antenna, as shown in Fig. 2. We query the tag at a rate of 5 Hz using Impinj Speedway Connect software [26]. The software operates at a frequency of 868 MHz with 32.5 dBm transmit power. We process RSSI readings through a moving average filter with a window size of 500 to produce the solid blue curve showing the average RSSI readings in Fig. 3. We simultaneously measure the surface temperature of the tag using an IR thermometer with ±2°C accuracy. The measured temperature is shown in the figure as a solid orange curve.

To compare the experimental results with the simulation, we extract a segment of the S_{22} curve from Fig. 1 (b). This curve segment is from the permittivity range of 77.4 to 69.5 that correspond to the measured temperature range of 27.9°C to 54.9°C, respectively. We plot the S_{22} curve segment as the dotted black line on the same figure against the same time coordinates for the horizontal axis as the measured temperature. Both the average RSSI curve and the S_{22} curve segment in Fig. 3 follow a similar trend and are close to each other. This behavior verifies the similar antenna performance in both the simulation and the experiment.

C. Mapping RSSI to temperature

Fig. 3 shows a tight relationship between the measured temperature and the average RSSI. This one-to-one mapping can estimate an unknown temperature for a given RSSI reading. In the following, we describe how we build our model to map a given RSSI reading to its corresponding temperature.

Since the ambient and initial temperatures are known, we use the least square method to fit the measured temperature $T_{\text{measured}}[t]$ for $t \in [0, \tau]$ (where τ is the timestamp of the last temperature measurement) to a Newton's cooling curve following (2) for an optimum k value k_{opt} as follows:

$$\min_{k} \sum_{t=0}^{\tau} \left\| \left[T_a + (T_0 - T_a)e^{kt}\right] - T_{\text{measured}}[t] \right\|^2 \rightarrow k_{\text{opt}} \quad (3)$$

We substitute k_{opt} derived from (3) with k in (2) to produce the optimum cooling curve $T_{\text{opt}}[t]$. We plot $T_{\text{opt}}[t]$ as the dashed orange curve in Fig. 3.

Let the set of average RSSI readings be $R[t]$ for $t \in [0, \tau]$ and $0 \leq \tau' \leq \tau$ where τ' is a timestamp between the initial and the final temperature readings. We use the least square method to superimpose $R[t]$ fully (when $\tau' = 0$) or partially (when $\tau' > 0$) over $T_{\text{opt}}[t]$ as follows:

$$\begin{aligned} \min_{\tau' \in [0,\tau]} \quad & \sum_{t=\tau}^{\tau' \rightarrow 0} \|R[t] - T_{\text{opt}}[t]\|^2 \\ \text{s.t.} \quad & |R[\tau'] - T_{\text{opt}}[\tau']| \leq \delta \end{aligned} \quad (4)$$

The constraint in (4) attempts to expand the overlapping region to as many time samples as possible. The factor δ corresponds to a 2°C accuracy on the temperature axis to give enough margin to extend the supporting temperature range. Subject to given constraints, Fig. 3 shows that $T_{\text{opt}}[t]$ follows $R[t]$ tightly over the whole temperature range. Once we establish the mapping model $R[t] \rightarrow T_{\text{opt}}[t]$, for a given RSSI value we can look up the corresponding temperature with an accuracy up to 2°C. This calibrated mapping is specific to the container and its content. Each tag undergoes per-tag calibration before put into use as done in state of the art [5].

Patch antennas are made of metal. Metal expands when heated and this slightly changes antenna dimensions. We conduct an experiment to investigate the impact of heat on the RFID tag. We use a similar setup as in [27] to heat up an RFID tag using an IR lamp and measure RSSI continuously. The results show no RSSI variation similar to the results in Fig. 3 throughout the experiment. Hence the local temperature of the tag antenna does not influence the antenna performance.

The simulation results in Fig. 1 show a significant difference in performance in RFID antennas when the surface permittivity changes. The experimental results in Fig. 3 verify the simulation results for different permittivity levels in water corresponding to different temperatures. We combine antenna performance in terms of RSSI with permittivity in terms of temperature to build a mapping model that relates average RSSI readings to a temperature with an accuracy of 2°C.

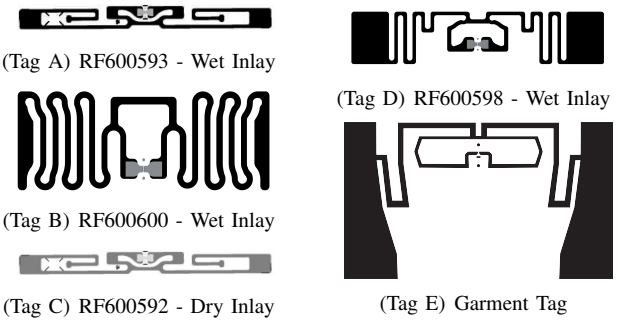

(Tag A) RF600593 - Wet Inlay

(Tag B) RF600600 - Wet Inlay

(Tag C) RF600592 - Dry Inlay

(Tag D) RF600598 - Wet Inlay

(Tag E) Garment Tag

Fig. 4. Different commodity RFID tag models used in the experiments.

IV. Experiments

Different commodity RFID tags have different antenna patterns. This makes them exhibit distinct antenna performances. Fig. 4 shows five commodity RFID tags with four different antenna patterns. We experiment with these five tag models to investigate how well they perform with our method.

A. Multiple tag models

Different RFID tag models have antenna patterns with different dimensions. They interact differently with the surface resulting in varying antenna performance. Hence they produce distinct RSSI patterns even in identical setups. We investigate how RSSI patterns from different tag models follow along the cooling curves to evaluate the performance of our method.

Tag A to Tag D in Fig. 4 are from the same manufacturer and Tag E is from a garment price tag with an unknown manufacturer. Wet inlays have an adhesive medium making them thinner stickers compared to dry inlay tags with a paper medium. The effective permittivity is different in different inlay types and hence they may have distinct RSSI patterns.

The experimental setup is as follows. We place a glass bottle with a pasted RFID tag in front of the antenna at a distance of 30 cm as shown in Fig. 2. The bottle is filled with 80°C hot water. The RFID reader queries the tag continuously at a rate of 5 Hz until the bottle cools down to the room temperature of 22°C. Simultaneously, we measure the surface temperature of the tag using an IR thermometer with ±2°C accuracy. We log both tag queries and temperature readings on the same computer concurrently. Since the IR thermometer readings fluctuate, we record 4-6 readings for 5 seconds and use the average temperature as the corresponding temperature. We use two bottles with two different tag models simultaneously to speed up the long data collection step. We repeat the same process three turns for each tag model.

Fig. 5 presents the results for a single measurement turn for each tag model introduced in Fig. 4. The solid orange curve with error bars represent the measured temperature. The top and bottom of an error bar corresponds to the highest and the lowest recorded temperature within the 5 second measurement period. The black bar chart at the bottom of each plot is the relative absolute difference between the average RSSI curve in the solid blue curve and the optimum cooling curve in the dashed orange curve. We normalize and scale the relative difference by a factor of 10 to visually enhance the magnitude.

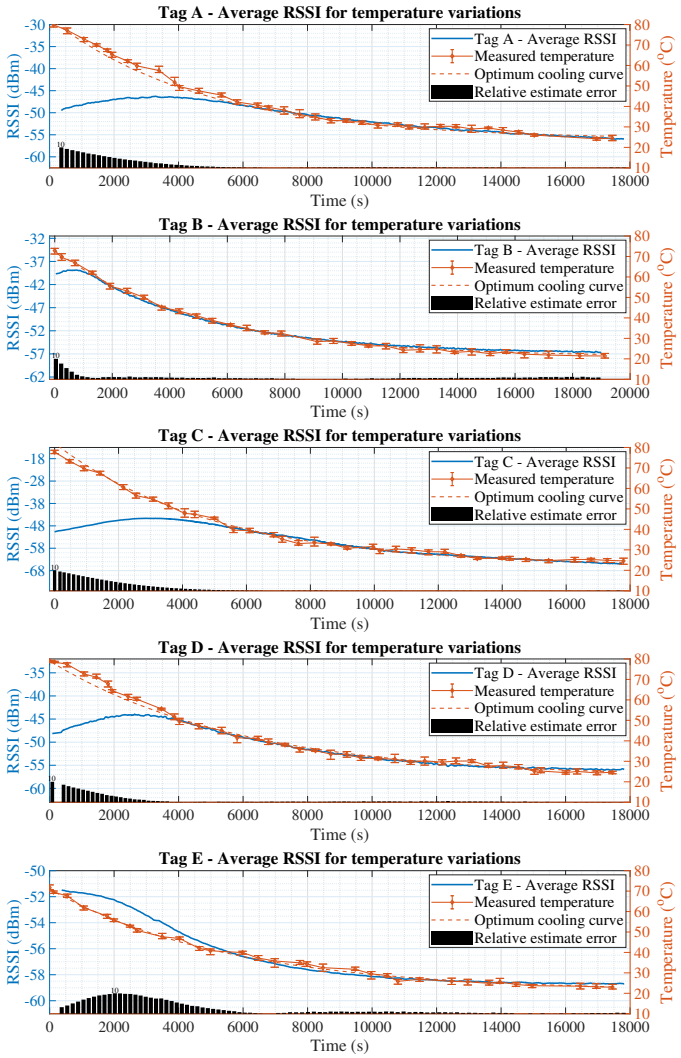

Fig. 5. RSSI variation of five different tag models with respect to temperature. All the tag models perform well with our model and closely follow a cooling curve to produce accurate temperature readings from RSSI measurements.

TABLE I
Average temperature estimate for multiple tag models

Tag Model	Temperature (°C)			
	Minimum	Maximum	Mean Error	Std. (σ)
Tag A	22.0	44.2	1.0	0.38
Tag B	22.0	60.0	1.5	0.37
Tag C	22.0	44.8	0.8	0.39
Tag D	22.1	50.3	1.1	0.68
Tag E	22.1	42.2	1.0	0.41

The resulting RSSI curve is different for each model in Fig. 5. However the RSSI pattern is similar for a tag model of the same type. Effective antenna length, effective surface area and material properties have an effect on the antenna performance with an S_{22} curve of a different scale. Hence the backscattered signal strength is different for different models.

Table I summarizes the average of results from all three measurement turns. The minimum and maximum recorded temperatures are under columns Minimum and Maximum

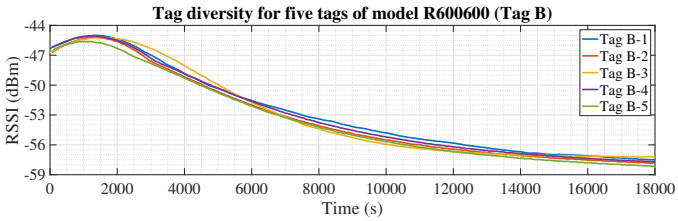

Fig. 6. Tag diversity. Variation of RSSI over time with respect to temperature changes for five identical RFID tags of the same model (Tag B - RF600600).

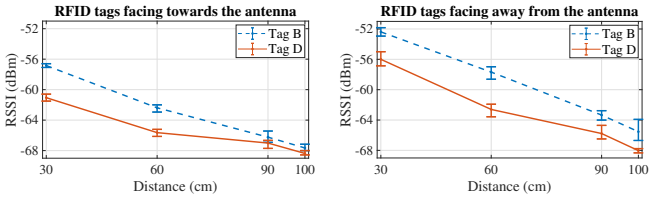

Fig. 7. RSSI variation of two RFID tags with varying distance and orientation.

respectively. Both these values suffice the constraints in (4) corresponding to a relative estimate error of 2°C. The mean error and the standard deviation define how distributed the average RSSI curve around the optimum cooling curve.

Although the RSSI curves are distinct, each tag model exhibits a similar antenna performance for varying temperatures. The steepness of an RSSI curve relates to the quality of the antenna matching in the presence of a surface with different permittivity. Tag B shows a much steeper RSSI curve compared to Tag A. Similar differences in performance are present in the advertised read ranges in the tag datasheets [22], [28]. Our method works up to 60°C as there is a lacking one-to-one mapping between RSSI and temperature when the RSSI curve diverges from the cooling curve at higher temperatures.

B. Tag diversity

Two RFID tags of the same model can have slight variations in dimensions of antenna traces. Such differences can cause slight changes in RSSI readings. This behavior helps fingerprinting RFID tags [29]. We investigate the antenna performance of five different RFID tags of the same model.

We experiment with five tags of Tag B model. Following the same setup as in Fig. 2, we carefully place one tag at a time and record the RSSI variation over time. Fig. 6 shows the shape and magnitude of the average RSSI variation of all five tags. All curves follow a similar trend with slight differences in magnitude. The average of the five curves also have similar attributes. Instead of modeling the RSSI to temperature mapping for individual tags, we can use a single mapping model based on this average of five RSSI curves for an identical setup and use it across multiple tags in the identical setup. However this will slightly affect the accuracy of the proposed method. Similar calibration steps to perform *one-shot calibration* are present in the state of the art [5].

C. Distance and direction

When not in direct line of sight, RFID tags could face any direction. We investigate how RSSI readings vary when tags

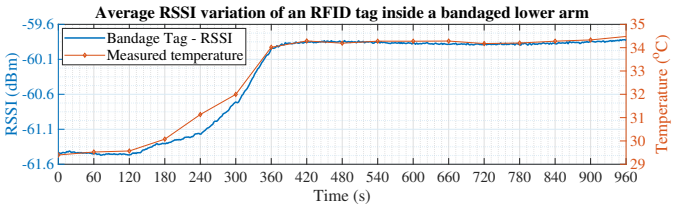

Fig. 8. RSSI variation of an RFID tag inside a bandaged lower arm. Bandage is first cooled down with an ice pack, before the body heat takes over.

face different directions and are at different distances from the reader antenna. We paste two RFID tags of models B and D on identical glass bottles filled with water at room temperature. The RFID reader makes 1000 queries per tag when the tags are facing towards and away from the antenna. Fig. 7 shows the average results of the experiment repeated three times for different tag-antenna distances. The signal strength decreases for both tags at increasing distances. We can leverage an accurate RFID localization technique in literature to measure the distance to the tag from the antenna [30] and calculate an offset for the RSSI to extend our method to different distances.

Fig. 7 also shows that the magnitude and the variance of the RSSI are higher when the tag face away. The water medium distorts the RF signals, causing a higher RSSI variation when the water medium is between the tag and the antenna. This limits the accuracy when tags face away from the antenna.

D. Limitations

Our method leverages RSSI measurements that are inherently noisy, in particular when there are changes in the environment. To handle this problem, we increase the number of RSSI samples and average them to improve accuracy and consistency at the expense of longer measurement time. In addition, we use COTS RFID readers and antennas to mitigate any potential multi-path effects and inconsistent RSSI measurements. Our method achieves high accuracy for materials with high permittivity variation like water, while materials with low variation lack comparable accuracy. So far, we have only measured temperatures above the ambient temperature, leaving lower temperature measurements to future work.

V. Applications

There are various use cases for temperature monitoring using commodity RFID tags. The following applications that require non-invasive, item-level temperature measurements show that our method is good enough even when the tags are not in direct line of sight with the RFID reader.

A. Monitoring body temperature

People with bandages or plaster casts need to keep the covered area still during the healing process. This may change the temperature under the covered body part. RFID tags are small and flexible enough to integrate inside the bandage and they can be safely used if the antenna is at least 50 cm away from the body [31]. We investigate the feasibility of our method to monitor temperature under a bandage complying to health directives with the informed consent of the volunteer.

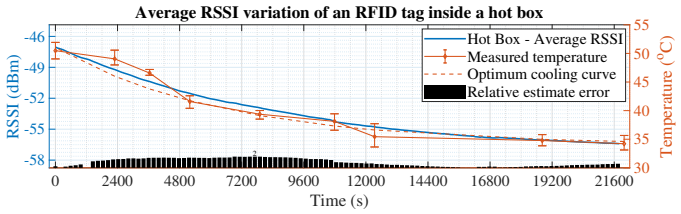

Fig. 9. Variation of RSSI of an RFID tag placed on a warm glass water bottle placed inside a heat insulated hot box. We measure the actual temperature of the bottle and tag using an IR thermometer by opening the box periodically.

Since the covered area is immobile, changes in RSSI will relate to changes in the temperature.

We place an RFID tag inside a bandage covering the lower arm. A digital thermometer records the ground truth temperature. We first cool the bandaged area to around 29°C using an ice pack and place it still, 80 cm away from the antenna. The RFID reader starts querying the RFID tag every half second until the body temperature takes over. We process the RSSI readings using a moving average filter with a window size of 4. Fig. 8 shows the resulting RSSI curve with corresponding body temperature. When the hand warms up, the RSSI rises and stables when the body temperature stables. This shows the applicability of our method in health-care monitoring applications that notify if there are temperature abnormalities.

B. Estimate food temperature in a hot box

Hot boxes keep food warm. We investigate if our method can accurately measure the temperature of a container inside a closed hot box. We place a glass bottle with 50°C hot water inside the hot box. The RFID tag on the bottle is facing towards the antenna. Fig. 9 shows the average RSSI curve during the experiment. It closely follows a cooling curve with 2°C accuracy. While using the IR thermometer to measure ground truth temperature, we open the hot box regularly. Some of the readings from the IR thermometer exceed 50°C. We discard such readings as they are invalid since they exceed the initial water temperature. Our method produces accurate results similar to the ground truth without direct line of sight unlike the IR thermometer that requires direct line of sight.

VI. Conclusion

This paper presents a non-invasive, item-level temperature sensing method using RSSI readings from a commodity RFID tag. We model the relationship between temperature and relative permittivity of a material in terms of RSSI. Our method achieves 2°C accuracy over a temperature range from 22°C to 60°C with 1.5°C mean error. We extend our experiments to five commodity RFID tag models to verify the proposed model. Our method enables various sensing applications ranging from logistic monitoring to health care that are otherwise hindered by power and accessibility constraints.

Acknowledgments

This work has been financially supported by the Swedish Research Council (Grant 2021-04968 and 2018-05480), and the Swedish Foundation for Strategic Research.

References

[1] Chester County Hospital, *Cast Care 101*. www.chestercountyhospital.org/news/health-eliving-blog/2019/august/cast-blog-article.
[2] National library of Medicine, *Temperature*. https://www.ncbi.nlm.nih.gov/books/NBK331/.
[3] M. L. Gavin MD., *Formula Feeding FAQs*. https://kidshealth.org/en/parents/formulafeed-storing.html.
[4] H. D. Young and R. A. Freedman, *Sears and Zemansky's University Physics with Modern Physics*. Harlow: Pearson Education Limited, 13th ed., 2012.
[5] X. Chen *et al.*, "Thermotag: Item-Level Temperature Sensing with a Passive RFID Tag," in *Proc. MobiSys '21*, (NY, USA), 2021.
[6] Impinj, *Types of RFID Systems*. https://www.impinj.com/products/technology/how-can-rfid-systems-be-categorized.
[7] R. Want, "An introduction to RFID technology," *Pervasive Computing, IEEE*, 2006.
[8] U. Ha, Y. Ma, Z. Zhong, T.-M. Hsu, and F. Adib, "Learning Food Quality and Safety from Wireless Stickers," in *Proc. of the 17th ACM Workshop on Hot Topics in Networks*, HotNets '18, (NY, USA), 2018.
[9] Avery Dennison, *Temperature Sensor Dogbone*. rfid.averydennison.com/content/dam/rfid/en/products/rfid-products/data-sheets/datasheet-Temperature-Sensor-Dogbone.pdf.
[10] RFMicron Corp., *RFM3200 Flexible Temperature Sensor*. https://www.impinj.com/products/technology/how-can-rfid-systems-be-categorized.
[11] S. Capdevila, L. Jofre, J. Romeu, and J. Bolomey, "Passive RFID based sensing," in *IEEE RFID-Technologies and Applications*, 2011.
[12] J. Wang, O. Abari, and S. Keshav, "Challenge: RFID Hacking for Fun and Profit," in *Proc. MobiCom '18*, 2018.
[13] S. Pradhan and L. Qiu, "RTSense: Passive RFID Based Temperature Sensing," in *ACM SenSys*, (New York, USA), 2020.
[14] Y. Shafiq *et al.*, "A Reusable Battery-Free RFID Temperature Sensor," *IEEE Transactions on Antennas and Propagation*, 2019.
[15] X. Wang *et al.*, "RFThermometer: A Temperature Estimation System with Commercial UHF RFID Tags," in *IEEE International Conference on Communications (ICC)*, 2019.
[16] R. Bhattacharyya, C. Floerkemeier, and S. Sarma, "RFID tag antenna based temperature sensing," in *IEEE RFID*, 2010.
[17] A. Vaz *et al.*, "Full Passive UHF Tag With a Temperature Sensor Suitable for Human Body Temperature Monitoring," *IEEE Transactions on Circuits and Systems II: Express Briefs*, 2010.
[18] A. Bensky, "Chapter 3 - Antennas and Transmission Lines," in *Short-range Wireless Communication (Third Edition)* (A. Bensky, ed.), pp. 43–83, Newnes, third edition ed., 2019.
[19] Y. Fan *et al.*, "Microstrip antennas integrated with electromagnetic band-gap (ebg) structures: a low mutual coupling design for array applications," *IEEE Transactions on Antennas and Propagation*, 2003.
[20] A. Catenaccio, Y. Daruich, and C. Magallanes, "Temperature dependence of the permittivity of water," *Chemical Physics Letters*, 2003.
[21] Simulia Corp., "CST Studio Suite 2022." https://www.3ds.com/products-services/simulia/products/cst-studio-suite/.
[22] Avery Dennison, *RF600600*. https://rfid.averydennison.com/en/home/product-finder/ad-321.html.
[23] U. Besson, "The history of the cooling law: When the search for simplicity can be an obstacle," *Science & Education*, vol. 21, 2010.
[24] Y. Nagasaka and A. Nagashima, "Simultaneous measurement of the thermal conductivity and the thermal diffusivity of liquids by the transient hot-wire method," *Review of Scientific Instruments*, 1981.
[25] Alien Technology, *ALR-8611-AC*. https://www.prosign.dk/Alien/ALR-8611-C.pdf.
[26] Impinj, "Impinj Speedway Connect." https://support.impinj.com/hc/en-us/articles/202755278-Speedway-Connect.
[27] C. A. Boano *et al.*, "Templab: A testbed infrastructure to study the impact of temperature on wireless sensor networks," in *IPSN '14*, 2014.
[28] Avery Dennison, *RF600593*. https://rfid.averydennison.com/en/home/product-finder/ad-229.html.
[29] S. Chinnappa Gounder Periaswamy, D. R. Thompson, and J. Di, "Fingerprinting RFID Tags," *IEEE Transactions on Dependable and Secure Computing*, 2011.
[30] C. Li, L. Mo, and D. Zhang, "Review on UHF RFID Localization Methods," *IEEE Journal of Radio Frequency Identification*, 2019.
[31] M. Roberti, *Can RFID Be Harmful to the Human Body?* www.rfidjournal.com/question/does-uhf-rfid-pose-a-radiation-threat-to-people.